Journal of Alloys and Compounds 601 (2014) 154–157

Contents lists available at ScienceDirect

Journal of Alloys and Compounds

journal homepage: www.elsevier.com/locate/jalcom

Improved thermal stability of $[001]_c$ poled $0.24Pb(In_{1/2}Nb_{1/2})O_3$–$0.47Pb(Mg_{1/3}Nb_{2/3})O_3$–$0.29PbTiO_3$ single crystal with manganese doping

Yuling Wang [a,b], Enwei Sun [a], Wei Song [a], Wanchong Li [a], Rui Zhang [a,*], Wenwu Cao [a,c]

[a] Condensed Matter Science and Technology Institute, Harbin Institute of Technology, Harbin 150080, China
[b] Physical and Electrical Information Engineering Institute, Daqing Normal University, Daqing 163712, China
[c] Materials Research Institute, The Pennsylvania State University, University Park, Pennsylvania 16802, USA

ARTICLE INFO

Article history:
Received 3 November 2013
Received in revised form 25 February 2014
Accepted 26 February 2014
Available online 7 March 2014

Keywords:
Piezoelectric
PIN–PMN–PT
Thermal stability

ABSTRACT

The temperature dependence of dielectric, piezoelectric, and electromechanical coupling properties of 0.5 wt.% manganese-doped and undoped $[001]_c$-poled $0.24Pb(In_{1/2}Nb_{1/2})O_3$–$0.47Pb(Mg_{1/3}Nb_{2/3})O_3$–$0.29PbTiO_3$ (0.24PIN–0.47PMN–0.29PT) single crystals has been investigated. Compared to the undoped single crystal, the Mn-doped 0.24PIN–0.47PMN–0.29PT demonstrated higher level of coercive field (9.8 kV/cm), increased Curie temperature (187 °C), improved mechanical quality factor Q_m (196), decreased piezoelectric constant d_{33} and comparable electromechanical coupling factor k_{33}, indicating hardening effects caused by the manganese ion substitution. More importantly, it was found that the Mn substitution significantly enhanced temperature stabilities of k_{33}, d_{33} and Q_m, leading to 30–40 °C improvement of the usage temperature range. These results show the application potential of Mn-doped ternary PIN–PMN–PT single crystals for the high-temperature and high-power electromechanical devices.

1. Introduction

Ternary relaxor-based ferroelectric $xPb(In_{1/2}Nb_{1/2})O_3$–$(1-x-y)Pb(Mg_{1/3}Nb_{2/3})O_3$–$yPbTiO_3$ (PIN–PMN–PT) single crystals, with compositions near the morphotropic phase boundary, demonstrate much higher coercive fields and curie temperature with comparably high-level piezoelectric and electromechanical properties compared to their binary counterpart $(1-x)Pb(Mg_{1/3}Nb_{2/3})O_3$–$xPbTiO_3$ (PMN–PT) single crystals [1–6]. However, its mechanical quality factor is still far lower than that of hard PZT ceramics [7], which limits its applications for high power ultrasonic transducers, sensors and actuators.

Recently, numerous efforts have been conducted to "harden" relaxor-PT single crystals through the addition of acceptor dopants, such as manganese (Mn) [8–13]. Through X-ray photoelectron spectroscopy (XPS) [8] and X-ray absorption fine structure (XAFS) analysis [9], the formation of oxygen vacancy dipole defects $(Mn_B'' - V_O^{\cdot\cdot})$ is observed in Mn-doped PMN-PT single crystals, which indicates the "harden effect" from Mn doping [10]. In ternary PIN–PMN–PT single crystals, Mn modification induces enhanced ferroelectric and pyroelectric properties [11], improved mechanical quality factor Q_m, and higher coercive field E_C, but a decrease in the piezoelectric and dielectric properties at room temperature [12,13]. In practical applications, the change of piezoelectric coefficient, electromechanical coupling factor, and mechanical quality factor with temperature will influence the performance of electromechanical devices. Therefore, understanding the temperature dependence of properties of Mn-doped ternary PIN–PMN–PT single crystals is very important.

In this work, we systematically investigated the temperature behavior of piezoelectric, dielectric, electromechanical properties and mechanical quality factor for both undoped and Mn-doped $[001]_c$-poled 0.24PIN–0.47PMN–0.29PT single crystals. Our results are useful for future development of high-power and high-temperature electromechanical devices based on these Mn-doped ternary single crystals.

2. Experimental

$[001]_c$-oriented undoped and 0.5 wt.% Mn-doped 0.24PIN–0.47PMN–0.29PT single crystals were supplied by H.C. Materials Corp, USA, which were grown by the modified Bridgman method [14,15]. X-ray diffraction (XRD) analysis was performed on both types of crystals. The dopant amount of Mn was determined to be ~0.5 wt.% by the scanning electron microscopy (SEM) with energy-dispersive X-ray spectroscopy, and the samples were oriented by the Laue machine with an accuracy of ±0.5°. Each sample was cut and polished into a parallelepiped with orientations of $[100]_c \times [010]_c \times [001]_c$ for $[001]_c$-poled crystals. In order to fill in the oxygen vacancies, the samples were annealed at 600 °C for 10 h, which also reduced the residual stress from crystal growth and mechanical processing.

* Corresponding author. Tel/fax.:+86 0451 86402797.
E-mail address: ruizhang_ccmst@hit.edu.cn (R. Zhang).

http://dx.doi.org/10.1016/j.jallcom.2014.02.174
0925-8388/

Afterwards, gold electrodes were sputtered onto the $[001]_c$ and $[00\bar{1}]_c$ samples surfaces. The samples were poled at a field of 15 kV/cm for 20 min in silicone oil at room temperature. The poling completeness of each sample was checked by a ZJ-2 piezo d_{33} meter.

The temperature dependence of dielectric properties was measured from room temperature up to 250 °C at a rate of 1 °C/min at the frequencies of 1 kHz, 10 kHz, and 100 kHz for both types of single crystals using an Agilent E4980A precision LCR meter. The dielectric constant was calculated from the measured capacitance based on the parallel capacitance approximation. The *P–E* hysteresis loops were measured on $[001]_c$-oriented plate samples from room temperature to 210 °C by the Precision Premier II (Radiant Technologies). In the thermal behavior measurements, a small amount of high-temperature conductive silver was employed as the electrode, and thin silver wires were attached for minimizing clamping effects on the samples. The thermal characteristics of piezoelectric, electromechanical characteristics and mechanical quality factor were determined by combining the Agilent 4294A Precision Impedance Analyzer with a heating-cooling optical stage (Thmse600, Linkam).

3. Results and discussion

The main properties of $[001]_c$-poled undoped and Mn-doped 0.24PIN–0.47PMN–0.29PT single crystals at room temperature are listed in Table 1. The dielectric constant $\varepsilon_{33}/\varepsilon_0$ and piezoelectric coefficient d_{33} decrease in Mn-doped samples, but the electromechanical coupling factor k_{33} of Mn-doped ternary samples maintains comparable level with that of the undoped crystal. More importantly, Mn-doped single crystal has much higher mechanical quality factor Q_m than the undoped sample (196 *vs.* 66).

Fig. 1 shows the temperature dependent *P–E* hysteresis loops of the two specimens. At room temperature, the Mn addition leads to the increase in both the remnant polarization P_r (from 23.6 μC/cm^2 to 26.5 μC/cm^2) and coercive field E_C (from ~5.8 kV/cm to ~9.8 kV/cm). Moreover, Mn doped PIN–PMN–PT single crystal also has better ferroelectric properties than that of undoped single crystal. This implies that the introduction of Mn ions into the 0.24PIN–0.47PMN–0.29PT single crystal produces a "hardening" effect [16]. As a result, the Mn-doped single crystal is more suitable for high-power electromechanical devices, such as underwater projectors and piezoelectric motors [17].

The XRD spectrum of undoped and Mn-doped 0.24PIN–0.47PMN–0.29PT single crystals, with corresponding diffraction indices, is shown in the inset of Fig. 2a. Clearly, both single crystals have rhombohedral symmetry with perovskite structure. In addition, Fig. 2 presents the dielectric constants ($\varepsilon_{33}/\varepsilon_0$) and dielectric loss as a function of temperature for $[001]_c$ poled undoped and Mn-doped 0.24PIN–0.47PMN–0.29PT single crystals at the frequencies of 1 kHz, 10 kHz and 100 kHz. The ferroelectric phase transition temperature T_{R-T} (rhombohedral to tetragonal) and Curie temperature T_C (tetragonal to cubic) were determined according to the locations of the dielectric permittivity peaks (at 1 kHz). For undoped single crystal, the T_{R-T} and T_C were found to be 102 °C and 145 °C, respectively, while in Mn-doped crystal, both transition temperatures increased noticeably ($T_{R-T} \sim 109$ °C and $T_C \sim 187$ °C, respectively). In addition, the dielectric loss is obviously lower for the Mn modified crystal, especially in the range from room temperature to T_{R-T}. In acceptor doped crystals, Mn ions substitute the *B* sites (Zr^{4+}/Ti^{4+}) of the perovskite structure due to the match of ionic radius, while oxygen vacancies can be generated due to valance mismatch. Thus, defect dipole pairs are developed inside the modified crystal, which leads to domain wall pinning and suppression of the dielectric and piezoelectric responses

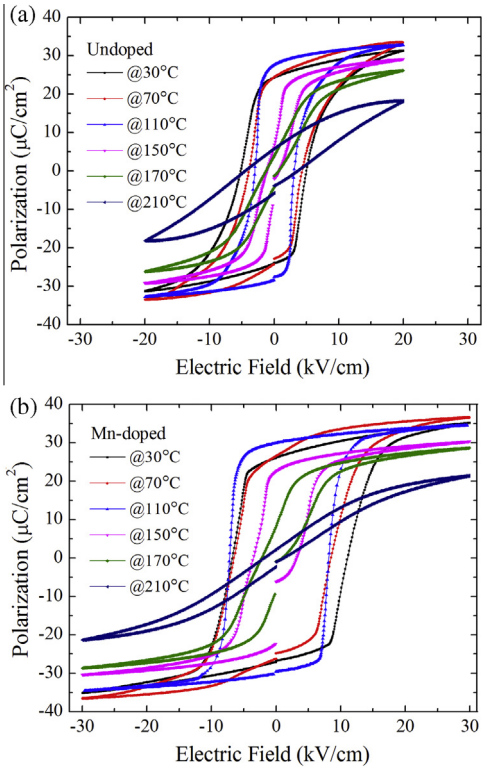

Fig. 1. Temperature dependence of *P–E* hysteresis loops in (a) undoped and (b) Mn-doped $[001]_c$-oriented 0.24PIN–0.47PMN–0.29PT single crystals.

[18,19]. These dipolar defects can provide nucleation centers for the ferroelectric phases, so that the phase transition temperatures are increased. At the same time, the suppression of the mobility of domain walls by the dipolar defects enhances the relaxation time, which lowers the losses [10,18].

Temperature stabilities of the longitudinal electromechanical coupling factor k_{33} for the undoped and Mn-doped crystals are shown in Fig. 3. The k_{33} value was determined based on the impedance spectrum at each temperature, and four representative impedance spectra are shown in the inset of Fig. 3. Clearly, the frequency difference between the resonant peak and the anti-resonant peak is reduced as the temperature increases. The k_{33} values in both crystals show little change when the temperature is lower than their respective T_{R-T}. In the undoped sample, k_{33} decreases sharply after T_{R-T} (~102 °C) due to the partial depolarization in the tetragonal phase, and reduces to zero at 170 °C. On the contrary, only a slow decrease was observed for the Mn-doped crystal even at temperatures higher than its T_{R-T} (close to 110 °C). The k_{33} value decreases to 0.73 at 140 °C, which is still higher than that of hard piezoelectric ceramics [20]. These results indicate a more stable electromechanical coupling characteristic for Mn-modified PIN–PMN–PT single crystal.

The temperature behaviors of the piezoelectric coefficient d_{33} in these two crystals are shown in Fig. 4. One can see that the d_{33} increases with temperature and reaches the peak value at T_{R-T} in the undoped crystal. The Mn-doped crystal shows a much slower

Table 1
Important physical properties of undoped and Mn-doped 0.24PIN–0.47PMN–0.29PT single crystals at room temperature.

PIN–PMN–PT	d_{33} (pC/N)	k_{33}	$\varepsilon^T_{33}/\varepsilon_0$ at 1 kHz	$\tan\delta$ (%) at 1 kHz	s^D_{33} (10^{-12} m^2/N)	s^E_{33} (10^{-12} m^2/N)	E_C (kV/cm)	Q_m
Undoped	1215	0.90	4553	0.56	10.95	48.33	5.8	66
Mn-doped	836	0.87	2635	0.40	12.20	36.64	9.8	196

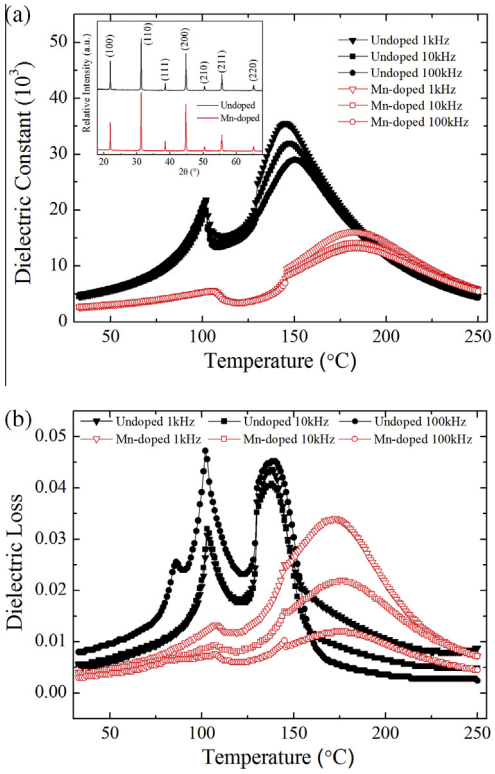

Fig. 2. Dielectric constant (a) and dielectric loss (b) as a function of temperature for $[001]_c$-poled undoped and Mn-doped 0.24PIN–0.47PMN–0.29PT single crystals. Inset: X-ray powder diffraction spectrum at room temperature with corresponding diffraction indices.

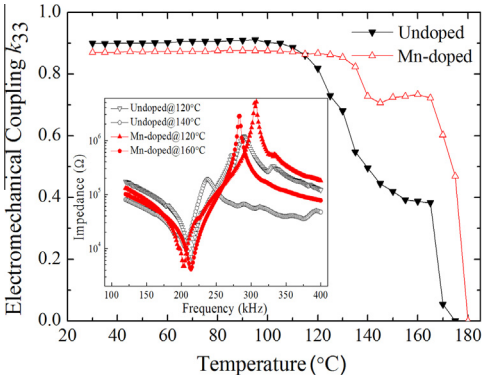

Fig. 3. Electromechanical coupling factor k_{33} as a function of temperature for $[001]_c$-oriented undoped and Mn-doped 0.24PIN–0.47PMN–0.29PT single crystals. The small inset shows the impedance spectra measured at different temperatures.

increasing trend than that of undoped crystal, indicating better temperature stability due to Mn substitution. Above T_{R-T}, d_{33} presents a fluctuant profile, which is caused by the depinning of domain walls due to temperature increase, and d_{33} decreases to zero at about 170 °C and 180 °C, respectively, for undoped and Mn-doped crystals. We notice that the dielectric peak values and the piezoelectric peak values are different in these domain-engineered single crystal samples. This is due to the fact that piezoelectric properties are directly related to the poling status of the crystal, while the dielectric peak is directly related to the phase transition. There is a dielectric peak even when the sample is unpoled, for which the piezoelectric constant is zero.

Furthermore, the thermal characteristic of the mechanical quality factor Q_m was investigated and shown in Fig. 5. Q_m was

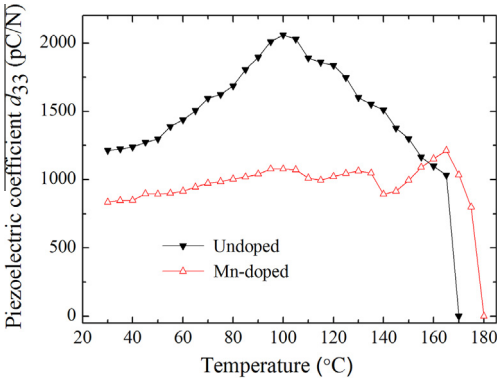

Fig. 4. Piezoelectric coefficient d_{33} as a function of temperature for $[001]_c$-oriented undoped and Mn-doped 0.24PIN–0.47PMN–0.29PT single crystals.

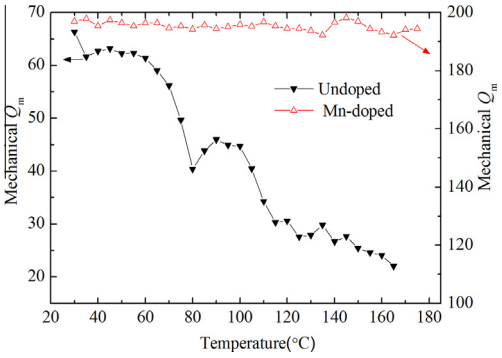

Fig. 5. Mechanical quality factor Q_m as a function of temperature for $[001]_c$-oriented undoped and Mn-doped 0.24PIN–0.47PMN–0.29PT single crystals.

computed by the formula: $Q_m = f_r/(f_1 - f_2)$ [21], where f_r is the resonance frequency, and f_1 and f_2 are frequencies at 3 dB down the maximum admittance. The Q_m of undoped specimen drops from 66 to 40 when the crystal is heated from room temperature to 80 °C. After a little increase around 100 °C (nearby its T_{R-T}), it decreases rapidly to zero at 165 °C. On the other hand, Q_m in Mn-substituted sample is nearly a constant up to 175 °C, indicating a significantly improved thermal stability due to Mn doping.

In the Mn-substituted crystal, a "hardening" effect is produced due to domain wall clamping and lattice stiffening, because an internal bias is induced from the development of acceptor-oxygen vacancy defect dipoles [22–24]. As a result, the piezoelectric constant, electromechanical coupling factor, and mechanical quality factor demonstrate better thermal stability compared to its undoped counterpart.

4. Summary and conclusions

The thermal behaviors of piezoelectric and electromechanical properties of ternary $[001]_c$-poled undoped and Mn-doped 0.24PIN–0.47PMN–0.29PT single crystals were studied. Compared to undoped crystals, although the longitudinal piezoelectric and electromechanical coupling factor at room temperature were decreased by the Mn substitution, the available temperature usage range of the crystal was enlarged by 30–40 °C. The Curie temperature, coercive field and mechanical quality factor were improved to 187 °C, 9.8 kV/cm, and 196, respectively. Moreover, the mechanical quality factor demonstrated better thermal stability due to the Mn doping. With these noticeably improved thermal stabilities of functional properties, the Mn-substituted ternary PIN–PMN–PT

crystals are more promising for electromechanical device applications at higher-temperatures and higher-driving field.

Acknowledgements

This research was supported in part by the National Key Basic Research Program of China (973) under Grant No. 2013CB6 32900, the National Natural Science Foundation of China of under Grant Nos. 50602009 and 11304061, Program of the Ministry of Education of China for New Century Excellent Talents in University under Grant No. NCET-06-0345, Postdoctoral Science Research Developmental Foundation of Heilongjiang Province under Grant No. LBH-Q06068, the Fundamental Research Funds for the Central Universities under Grant No. HIT.NSRIF.2014083, the China Postdoctoral Science Foundation under Grant No. 2013M531029, and the Daqing Normal University Youth Foundation No. 12ZR12.

References

[1] J. Tian, P. Han, X. Huang, H. Pan, J. Carroll III, D. Payne, Appl. Phys. Lett. 91 (2007) 222903.
[2] E. Sun, S. Zhang, J. Luo, T.R. Shrout, W. Cao, Appl. Phys. Lett. 97 (2010) 032902.
[3] Z. Wang, R. Zhang, E. Sun, W. Cao, J. Alloys Comp. 527 (2012) 101.
[4] Z. Feng, X. Zhao, H. Luo, J. Appl. Phys. 100 (2006) 024104.
[5] D. Lin, Z. Li, F. Li, Z. Xu, X. Yao, J. Alloys Comp. 489 (2010) 115.
[6] E. Sun, R. Zhang, F. Wu, W. Cao, J. Alloys Comp. 553 (2013) 267.
[7] S. Zhang, S. Lee, D. Kim, H. Lee, T. Shrout, Appl. Phys. Lett. 93 (2008) 122908.
[8] X. Wu, L. Liu, X. Li, Q. Zhang, B. Ren, D. Lin, X. Zhao, H. Luo, Y. Huang, J. Cryst. Growth 318 (2011) 865.
[9] X. Li, X. Zhao, B. Ren, H. Luo, W. Ge, Z. Jiang, S. Zhang, Scr. Mater. 69 (2013) 377.
[10] L. Luo, M. Dietze, C.H. Solterbeck, H. Luo, M. Es-Souni, J. Appl. Phys. 114 (2013) 224112.
[11] L. Li, X. Li, X. Zhao, B. Ren, Q. Xu, H. Xu, H. Luo, X. Li, X. Shao, J. Alloys Comp. 595 (2014) 120.
[12] X. Huo, S. Zhang, G. Liu, R. Zhang, J. Luo, R. Sahul, W. Cao, T.R. Shrout, J. Appl. Phys. 113 (2013) 074106.
[13] L. Zheng, R. Sahui, S. Zhang, W. Jiang, S. Li, W. Cao, J. Appl. Phys. 114 (2013) 104105.
[14] Z. Yin, H. Luo, P. Wang, G.S. Xu, Ferroelectrics 229 (1999) 207.
[15] J. Tian, P. Han, X. Huang, H. Pan, J.F. Carroll III, D.A. Payne, Appl. Phys. Lett. 91 (2007) 222903.
[16] S. Takahashi, Ferroelectrics 41 (1982) 143.
[17] N. Sherlock, S. Zhang, J. Luo, H. Lee, T. Shrout, R. Meyer, R. Jr, J. Appl. Phys. 107 (2010) 074108.
[18] S. Priya, K. Uchino, J. Appl. Phys. 91 (2002) 4515.
[19] E. Sun, R. Zhang, F. Wu, B. Yang, W. Cao, J. Appl. Phys. 113 (2013) 074108.
[20] T. Shrout, S. Zhang, J. Electroceram. 19 (2007) 111.
[21] S. Priya, K. Uchino, D. Viehland, Jpn. J. Appl. Phys. 40 (2001) L1044. Part 2.
[22] S. Zhang, J. Luo, W. Hackenberger, N. Sherlock, R. Jr, T. Shrout, J. Appl. Phys. 105 (2009) 104506.
[23] P. Finkel, C. Murphy, J. Stace, K. Bussmann, A. Heitmann, Appl. Phys. Lett. 102 (2013) 182903.
[24] A. Amin, H.Y. Lee, B. Kelly, Appl. Phys. Lett. 90 (2013) 242912.